

Solvent Effects on the Structural, Electronic, Non-Linear Optical and Thermodynamic Properties of Perylene Based on Density Functional Theory

Abstract:

7 Perylene ($C_{20}H_{12}$) is an important member of the polycyclic aromatic hydrocarbons (PAHs) that
8 has a wide **applications such as organic photovoltaic cells, field effect transistors and biosensors.**
9 Optimized bond lengths and bond angles, HOMO-LUMO energy gap, global chemical indices,
10 total energy, nonlinear optical and thermodynamic properties of Perylene in the gas phase and in
11 solvents (water, chloroform, benzene and acetone) were obtained based on Density Functional
12 Theory with B3LYP/6-311++G(d,p) basis set. All the computations were carried out using
13 Gaussian 03 **package** and revealed that the solvents have an effect on the optimized parameters.
14 It was observed that the bond lengths increase with an increase in the polarity of the solvents,
15 while the bond angles were found to increase as the polarity of the solvents decreases. **Perylene**
16 **molecule was found** to have a higher stability in the gas phase with HOMO-LUMO energy gap
17 of 2.9935eV. The HOMO and HOMO-LUMO energy gap were found to increase with an
18 increase in polarity of the solvents. The molecule was found to be harder and less reactive in the
19 gas phase with chemical hardness of 1.4968eV. The maximum value of ionization potential
20 5.3227eV and minimum value of electron affinity 2.2757eV were obtained in water **and gas**
21 **phase respectively**, as such it is difficult to remove an electron from the molecule in water to
22 form an ion and it is also difficult to add an electron to the molecule **in gas phase**. The ground
23 state total energy of the molecule was found to increase with an increase in polarity of the
24 **solvents**. Similarly, the **chemical** hardness, chemical softness, electronegativity, chemical
25 potential and electrophilicity index were found to increase with an increase in the dielectric
26 constant of the solvents. In the non-linear optical (NLO) properties calculations, it was observed
27 that Perylene is a neutral molecule. It was found that the specific heat capacity of perylene
28 increases with an increase in the polarity of the solvent while the entropy and the zero-point
29 vibrational energy of the molecule decreases as the polarity of the solvent increases. In the non-
30 linear optical properties calculations, it was found that the polarizability ($\langle\alpha\rangle$) of Perylene
31 increases with decrease in the polarity of the solvents and the anisotropic polarizability ($\Delta\alpha$) of
32 Perylene increase with an increase in the polarity of the solvents. In the Natural Bond Orbital
33 (NBO) analysis, high intensive interaction between donor and acceptor electrons of Perylene was
34 **observed in chloroform due to** large stabilization energy of 4.49Kcal/mol. The result shows
35 that careful selection of the solvents and basis sets can tune the frontier molecular **molecular**
36 **orbital energy gap**.

KEYWORDS: Density Functional Theory, Gaussian 03, HOMO-LUMO, Non-linear Optical Properties and Perylene.

39

40 **1. INTRODUCTION**

41 With rising demand for sustainably risk free energy, there is no better alternative than organic
42 electronic materials which have proved to be a promising candidates for advanced optoelectronic
43 applications such as in light emitting diodes, photovoltaic cells [1], organic field effect
44 transistors, organic solar cells and transparent white displays [2, 3]. To fully understand and use
45 these materials, their basic fundamental physical properties must be sufficiently explored. To
46 acquire such vital information, their structural, electronic, optical, non-linear optical and
47 thermodynamic properties are required.

48 Rylene are series of polycyclic aromatic hydrocarbons (PAHs) with general chemical formula
49 $C_{10n}H_{4n+4}$ among which are the most widely investigated perylene ($C_{20}H_{12}$) and its derivatives
50 such as pyrenebisimides, perylene tetracarboxylic acid (PTDCA) and perylene-3,4,9,10-
51 tetracarboxylic anhydride (PDA) which, due to their promising electronic, optical and charge-
52 transport properties, are widely used in high-tech applications such as organic photovoltaic,
53 organic field effect transistors, biolabels, sensors, single molecular spectroscopy, super
54 molecular assemblies and opto-electronic devices [4].

55 Interestingly, wide ranges of experimental and theoretical studies have explored the synthesis
56 and applications of perylene and its derivatives including Density Functional Theory. For
57 instance, [5] presented within the framework of Density Functional Theory (DFT) as well as a
58 comparative study of the electronic, optical, and transport properties of some selected polycyclic
59 aromatic hydrocarbons (Perylene included). Similarly, the structural, and optoelectronic
60 properties of different classes of of perylene: isolated perylene, diindo[1,2,3-cd:1',2',3'-
61 Im]perylene (DIP) molecule and DIP molecular crystal were investigated [6]. The effect of
62 aggregation on the excited-state electronic structure of Perylene through transient absorption
63 measurements of isolated molecules, excimers in solution, monomeric crystal forms (β -
64 perylene), and dimeric crystal forms (α -perylene) were studied [7]. The aggregation of water
65 soluble, dicationic Perylene bisimide derivatives using absorption and emission spectroscopies,
66 X-ray and neutron scattering techniques as well as electron microscopy, provides evidence for
67 the existence of higher order molecular aggregates in solution [2]. The structure and electronic

68 properties of pyrelene and coronene under pressure were also theoretically investigated using
69 DFT [8] and Van der Waals interaction which were also used in obtaining the electronic structure
70 of crystalline perylene [9]. However, to the best of our knowledge, the effects of solvents on this
71 promising organic material have never been studied before. In the present investigation,
72 computational studies have been carried out to investigate the effects of solvents on the
73 structural, electronic, thermodynamic and non-linear optical properties of Perylene based on
74 density functional theory.

75 Choice of a suitable solvent is of paramount scientific interest to obtain desired efficiency,
76 selectivity and kinetics of chemical reaction [10]. The solvents used in this work include Water,
77 Chloroform, Benzene and Acetone with the following dielectric constants; Water ($\epsilon = 80.37$),
78 Chloroform ($\epsilon = 4.806$), Benzene ($\epsilon = 2.284$) and Acetone ($\epsilon = 37.50$).

79 2. THEORETICAL BACKGROUND

80 2.1 Density Functional Theory

81 Density Functional Theory is a phenomenally successful approach to finding solutions to the
82 fundamental equation that describes the quantum behavior of atoms and molecules [11]. DFT has
83 proved to be highly successful in describing structural and electronic properties in a vast class of
84 materials, ranging from atoms and molecules to simple crystals to complex systems [12]. Density
85 functional theory (DFT) was proposed by Hohenberg and Kohn as a method to determine the
86 electronic structure of a system at ground state with a theory stating that all ground state
87 properties for many particle systems are functional of the electron density [13, 14]. In 1965,
88 Kohn and Sham (KS) reformulated the problem in a more familiar form and opened the way to
89 practical application of DFT [12]. For a system of non- interacting electrons, the ground state
90 charge density is representable as a sum over one-electron orbitals (KS orbitals) $n(r)$ [12]. That
91 is;

$$92 \quad n(r) = 2 \sum_i |\Psi_i(r)|^2 \quad (1)$$

93 If we assume double occupancy of all states, and the Kohn-Sham orbitals are the solution to the
94 Schrodinger equation.

95
$$\left[-\frac{\hbar^2}{2m} \nabla^2 + V_{KS}(r) \right] \Psi_i(r) = \epsilon_i \Psi_i(r) \quad (2)$$

96 where,

97
$$V_{KS} = V_{ext} + \int \frac{e^2 n(r) n(r')}{|r-r'|} dr dr' + V_{XC}[n(r)] \quad (3)$$

98 is a unique potential having $n(r)$ as its charge density. Thus we have;

99
$$\left(-\frac{\hbar^2}{2m} \nabla^2 + V_H(r) + V_{XC}[n(r)] + V(r) \right) \Psi_i(r) = \epsilon_i \Psi_i(r) \quad (4)$$

100 where, $V_H(r)$ is the Hartree potential and $V_{XC}[n(r)]$ is the exchange correlation potential.

101 A wide variety of different approximations have been developed to take care of the effects of
 102 electron-electron interactions such as the generalized gradient approximation (GGA), local
 103 density approximation (LDA) and Hybrid Approximations.

104 In the LDA, the exchange correlation energy at a point in space is taken to be that of the
 105 homogeneous electron gas with local-density $\epsilon_{XC}(n)$. Thus the total exchange correlation
 106 energy functional is approximated as [15];

107
$$E_{XC}^{LD} = \int n(r) \epsilon_{XC}(n(r)) dr \quad (5)$$

108 From which the potential is obtained as;

109
$$V_{XC} = \frac{\delta E_{XC}}{\delta n} \quad (6)$$

110 where, δE_{XC} and δn are the derivatives of the exchange energy and the electron density
 111 respectively.

112 Whereas, the generalized gradient approximation (GGA) depends on both local density and it's
 113 gradient, it can be expressed as;

114
$$E_{XC}^{GGA} = \int n(r) \epsilon_{XC}(n|\nabla n|\nabla^2 n) dr \quad (7)$$

115 where, $n(r)$ is the electron density.

116 Unlike LDA and GGA, the hybrid function is a linear combination of Hartree-Fock exchanges
117 expressed as [15]:

118
$$E_{XC}^{hybrid} = \alpha E_{XC}^{HF} + E_C \quad (8)$$

119 where E_{XC}^{HF} is the Hartree-Fock exchange energy and α can be chosen to satisfy particular criteria.

120 **2.2 Global Quantities**

121 Global reactivity descriptors such as chemical potential, chemical hardness-softness,
122 electronegativity and electrophilicity index are useful quantities in predicting and understanding
123 global chemical reactivity trends. The ionization potentials (IP) and electron affinities (EA) of
124 the molecule in the gas phase and in solvents are computed using Koopman's Hypothesis,
125 through the HOMO and LUMO energy orbitals respectively using the following expressions;

126
$$IP = -E_{HOMO} \quad (9)$$

127
$$EA = -E_{LUMO} \quad (10)$$

128 The difference between the highest occupied molecular orbital (HOMO) and lowest unoccupied
129 molecular orbital (LUMO) known as energy gap can be obtained from the relation;

130
$$E_{gap} = E_{LUMO} - E_{HOMO} \approx IP - EA \quad (11)$$

131 Chemical hardness is given by half of the energy band gap [16];

132
$$\eta = \frac{IP - EA}{2} \quad (12)$$

133 The softness of a molecule can be obtained by taking the inverse of its chemical hardness [17];

134
$$S = \frac{1}{\eta} \quad (13)$$

135 The chemical potential is given by [17];

136
$$\mu = -\left(\frac{IP + EA}{2}\right) \quad (14)$$

137 The electronegativity is given by [17];

138
$$\chi = \frac{IP+EA}{2} \quad (15)$$

139 The electrophilic index is expressed as [17, 18];

140
$$\omega = \frac{\mu^2}{2\eta} \quad (16)$$

141 **2.3 Non-Linear Optical Properties**

142 In order to gain an insight on the effects of solvent on the non-linear optical properties (NLO) of
 143 **perylene; the dipole** moment, polarizability, anisotropic polarizability and hyperpolarizability
 144 were calculated.

145 Dipole moment is a property used in describing the polarity of a system. For molecular systems,
 146 this property can be obtained from[19];

147
$$\mu_{tot} = [\mu_x^2 + \mu_y^2 + \mu_z^2]^{1/2} \quad (17)$$

148 where μ_x , μ_y and μ_z are the components of the dipole moment in x, y and z coordinates.

149 Electric dipole polarizability is an important property used in determining the polarizability of a
 150 molecule or compound. It is a measure of the linear response of an infinitesimal electric field (F)
 151 and represents second-order variation energy [20];

152
$$\alpha = -\frac{\partial^2 E}{\partial F_a \partial F_b} \quad (18)$$

153 where a, and b are coordinates of x, y and z. The mean polarizability is calculated using [16];

154
$$\alpha = \frac{1}{3}(\alpha_{xx} + \alpha_{yy} + \alpha_{zz}) \quad (19)$$

155 where the α_{xx} , α_{yy} and α_{zz} quantities are known as principal values of polarizability tensor.

156 The anisotropic polarizability is given by [17]:

157
$$\Delta\alpha = \left[\frac{(\alpha_{xx} - \alpha_{yy})^2 + (\alpha_{yy} - \alpha_{zz})^2 + (\alpha_{zz} - \alpha_{xx})^2 + 6(\alpha_{xz}^2 + \alpha_{xy}^2 + \alpha_{yz}^2)}{2} \right]^{1/2} \quad (20)$$

158 The mean first hyperpolarizability is defined as [17, 21]:

159
$$\beta_{tot} = (\beta_x^2 + \beta_y^2 + \beta_z^2)^{1/2} \quad (21)$$

160 where β_x , β_y and β_z are defined as:

161
$$\beta_x = \beta_{xxx} + \beta_{xyy} + \beta_{xzz}$$

162
$$\beta_y = \beta_{yyy} + \beta_{xxy} + \beta_{yzz}$$

163
$$\beta_z = \beta_{zzz} + \beta_{xxz} + \beta_{yyz} \quad (22)$$

164 The β_x , β_y and β_z refer to the components of hyperpolarizability along x , y and z components of
165 molecular dipole moment.

166 2.4 Natural Bond Orbital (NBO)

167 NBO analysis provides an efficient method for studying intra and intermolecular bonding
168 interactions among bonds, and also provides a convenient basis for investigation of charge
169 transfer or conjugative interactions in molecular systems [22]. The second-order Fock matrix is
170 used to evaluate the donor-acceptor interactions in the NBO basis. For each donor and acceptor,
171 the stabilization energy $E^{(2)}$ associated with the electron delocalization between donor and
172 acceptor is estimated as [23];

173
$$E^{(2)} = -n_\sigma \frac{\langle \sigma | F | \sigma \rangle^2}{\varepsilon_{\sigma^*} - \varepsilon_\sigma} = -n_\sigma \frac{F_{ij}^2}{\Delta E} \quad (23)$$

174 where $\langle \sigma | F | \sigma \rangle^2$, or F_{ij}^2 is the Fock matrix element between i and j NBO orbitals, ε_{σ^*} and ε_σ are
175 the energies of σ^* and σ NBO's and n_σ is the population of the donor orbital.

176 3. COMPUTATIONAL METHOD

177 Geometry of perylene was optimized with no symmetry constraint using Becke's three-
178 parameter hybrid exchange [24] combined with Lee-Yang-Parr's gradient-corrected correlation
179 [25] functional (B3LYP) method with 6-311++G(d,p) basis set. All the parameters were fully
180 allowed to relax and each of the calculations converged to an optimized geometry which
181 corresponds to a true energy minimum.

182 For the study of solvation effects, a Self-Consistent Reaction Field (SCRF) approach based on
183 Polarizable Continuum Model (PCM) were employed. The effects of four solvents (water,
184 chloroform, benzene and acetone) were investigated by means of the SCRF method based on
185 PCM as implemented in the Gaussian 03 [26]. The optimized geometries were then used to
186 obtain the HOMO-LUMO energy gap, chemical hardness, chemical softness, chemical potential,
187 electronegativity, electrophilicity index, dipole moment, polarizability, anisotropic polarizability,
188 hyperpolarizability, entropy and the specific heat capacity of the investigated molecule at the
189 same level of theory (B3LYP/6-311++G(d,p)). Finally, the NBO calculations [27] were
190 performed using NBO 3.1 program as implemented in the Gaussian 03 package at same level of
191 theory in order to understand the various second-order interactions between the filled orbitals of
192 one subsystem and the vacant orbitals of another subsystem. All calculations were performed
193 within the framework of Density Functional Theory (DFT) as coded in Gaussian 03 package
194 [26].

195 **4. RESULTS AND DISCUSSION**

196 **4.1 Optimized Parameters**

197 The optimized values of bond lengths and bond angles of the studied molecule were calculated at
198 DFT/B3LYP level using 6-311++G(d,p) basis set in the gas phase and in different solvents
199 (water, chloroform, benzene and acetone). The results are shown in Tables 1 and 2. The distance
200 between the nuclei of two atoms bonded together is termed as bond length while bond angle is
201 the angle between two adjacent bonds of an atom in a molecule [20].

202 From Table 1, there are little changes in the bond lengths of Perylene when optimized with
203 water, chloroform, benzene and acetone compared with the gas phase. The result shows that the
204 lowest value obtained was 1.0825 \AA in benzene. However, when compared with results of an
205 isolated perylene molecule [6], the bond lengths here tend to be a little smaller. It is worth noting
206 that, the smaller the bond length, the higher the bond energy and stronger the bond [28].
207 Consequently, this has affirmed that the bond lengths of perylene in the gas phase and in solvents
208 are a little stronger than that of an isolated perylene molecule. Hence, an enormous amount of
209 energy is required to break these bonds. It was also observed that the bond length increases with
210 an increase in the polarity of the solvents.

211 **Table 1:** Selected bond lengths (\AA) of the optimized structure of perylene in the gas phase and in
 212 different solvents.

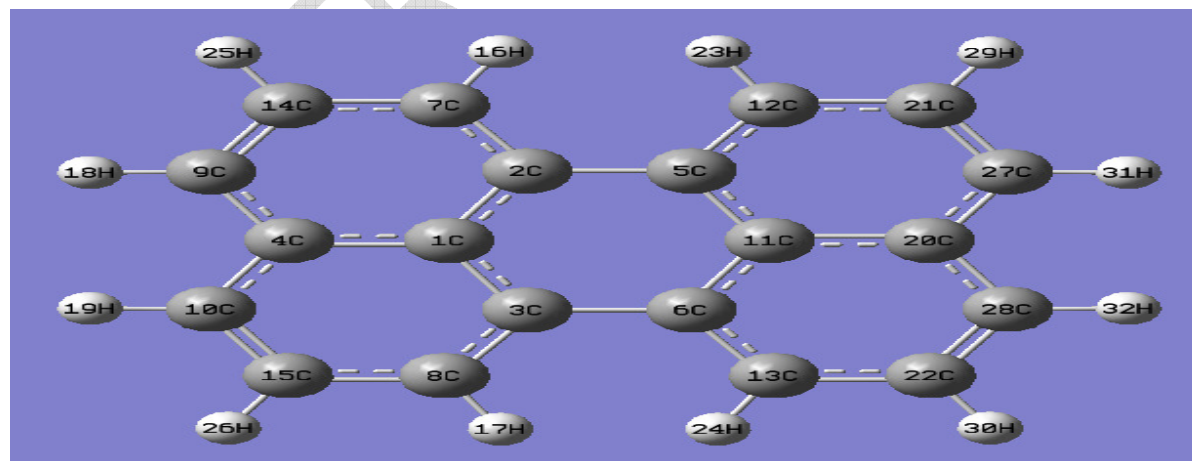
Bond Lengths (\AA)	Gas Phase	Water	Chloroform	Benzene	Acetone	Previous Work
R(2,5)	1.4762	1.4773	1.4769	1.4765	1.4772	1.4700 ^a
R(1,4)	1.4339	1.4346	1.4342	1.434	1.4345	1.4360 ^a
R(1,2)	1.4315	1.4324	1.4319	1.4316	1.4323	1.4310 ^a
R(28,32)	1.0858	1.0877	1.0866	1.0858	1.0875	1.0900 ^a
R(14,25)	1.0853	1.0872	1.0862	1.0854	1.087	1.0900 ^a
R(13,24)	1.0827	1.0846	1.0833	1.0825	1.0841	1.0900 ^a

213 ^a[6]

214 **Table 2:** Selected bond angles ($^{\circ}$) of the optimized structure of perylene in the gas phase and in
 215 different solvents.

Bond Angles ($^{\circ}$)	Gas Phase	Water	Chloroform	Benzene	Acetone
A(6,3,8)	122.184	122.106	122.130	122.143	122.119
A(3,8,15)	122.001	121.870	121.918	121.944	121.890
A(14,9,18)	120.748	120.919	120.866	120.838	120.900
A(11,20,27)	119.592	119.640	119.626	119.612	119.639
A(20,28,32)	118.965	118.859	118.894	118.905	118.876
A(14,7,16)	117.706	117.733	117.717	117.759	117.679

216



217

218 **Fig.1** Optimized Structure of Perylene

219 However, the longest bond length is 1.477 \AA , which is almost the same in both gas phase and
220 solvents. The structural geometry of the studied molecule that consists of bond lengths and bond
221 angles are found to be in good agreement with those from previous work [6]. But in [6] the
222 molecule is in the form of an isolated perylene, diindo[1,2,3-cd:1',2',3'- Im]perylene (DIP)
223 molecule and DIP molecular crystal.

224 **4.2 Frontier Molecular Orbital Energies (FMOEs)**

225 Table 3 presents the highest occupied molecular orbital (HOMO), the lowest unoccupied
226 molecular orbital (LUMO) and HOMO and LUMO energy gaps of perylene in the gas phase and
227 in solvents calculated at the DFT/B3LYP level in the 6-311++G(d,p) basis set. The values of
228 HOMO, LUMO and their energy gaps reflect the chemical activity of the molecule. The energy
229 gap between HOMO and LUMO determines the kinetic stability, chemical reactivity, optical
230 polarizability and chemical hardness-softness of a molecule [21]. Compounds with large
231 HOMO-LUMO gap value tend to have higher stability [18]. In this work, the order of stability of
232 the molecule is more in the gas phase > water > acetone > chloroform > benzene. Interestingly, the
233 order of stability increases with an increase in polarity of the solvents.

234 HOMO as an electron donor represents the ability to donate an electron, while LUMO as an
235 electron acceptor represents the ability to accept an electron. The smaller the LUMO and HOMO
236 gaps, the easier it is for the HOMO electron to be excited; the higher the HOMO energies, the
237 easier it is for HOMO to denote electrons; the lower the LUMO energies, the easier it is for the
238 LUMO to accept electrons [29].

239 It can be observed from Table 3, that the LUMO energy of perylene in benzene (-2.2829 eV) is
240 smaller than that in the gas phase and in the rest of the solvents. Hence, the electron transfer from
241 HOMO to LUMO of the molecule in benzene is relatively easier than that in the gas phase and in
242 the rest of the solvents. It can also be observed that the HOMO and energy gap of perylene
243 increases with increase in polarity of the solvents.

244 The HOMO-LUMO gap of 2.976 eV obtained in the gas phase is found to be very close to 2.972
245 eV of an isolated Perylene reported by [6].

246 **Table 3:** Calculated HOMO, LUMO and energy gap in (eV) of the optimized structure of
 247 perylene in the gas phase and different solvents using B3LYP methods with 6-311++G(d,p) basis
 248 set.

Solvents	E_{HOMO} (eV)	E_{LUMO} (eV)	Gap (eV)	Previous Work
Gas Phase	-5.2693	-2.2757	2.9935	2.9740 ^a 2.98 ^b
Water	-5.3227	-2.3332	2.9895	
Chloroform	-5.2878	-2.3005	2.9873	
Benzene	-5.2729	-2.2829	2.9860	
Acetone	-5.3167	-2.3274	2.9893	

249 ^a[6] ^b[5]

250 **4.3 Total Ground State Energy**

251 **Table 4** presents the dielectric constants of the solvents and total energy in atomic mass unit (a.u)
 252 of Perylene molecule in the gas phase and in different solvents calculated at the DFT/B3LYP
 253 level with 6-311++G(d,p) basis set. The ground state total energy is an important property that
 254 describes the physical properties of a molecule. It can be seen from **Table 4** that the ground state
 255 total energy increases with an increase in dielectric constant of the solvents.

256 **Table 4:** Ground state total energies in atomic mass unit (a.u) of the optimized structure of
 257 perylene in the gas phase and different solvents.

Solvents	B3LYP/6- 311++G(d,p)	ϵ
Gas Phase	-769.5611634	-
Water	-769.5983746	80.37
Chloroform	-769.5914965	4.806
Benzene	-769.5874674	2.284
Acetone	-769.5954100	37.50

258

259 **4.4 Ionization Potentials and Electron Affinity**

260 The ionization potential (IP) and electron affinity (EA) measure the tendency of compounds to
 261 lose or gain an electron [30]. The IPs and EAs are presented in Table 5. The higher the ionization

262 potential (IP), the more difficult it is to remove an electron to form an ion. The lower the electron
263 affinity (EA), the less easy it is to add an electron.

264 In Table 5, it can be observed that it is more difficult to remove an electron from water>
265 acetone> chloroform> benzene> gas phase to form an ion. Similarly, it is more difficult to add an
266 electron in terms of their EAs to the molecule in gas phase> benzene>chloroform> acetone
267 >water. It was observed that the ionization potential increases with an increase in the polarity of
268 the solvents while the electron affinity decreases as the polarity of the solvents decreases. Non-
269 polar hydrocarbon molecules such as perylene are hydrophobic (water fearing) in nature. Water
270 and some other polar solvents are unable to form significant attractive interactions with non polar
271 molecules in which the carbon and hydrogen atoms are well bonded together through non polar
272 vander waals interactions. In other words the energy derived from the interactions of polar
273 solvents and non polar organic molecule is not enough to breakup the ion-ion interaction within
274 the molecule.

275

276

277 **Table 5:** Ionization potentials and electron affinities of the optimized structure of a perylene
278 molecule in the gas phase and different solvents.

Solvents	IP (eV)	EA (eV)
Gas Phase	5.2693	2.2757
Water	5.3227	2.3332
Chloroform	5.2878	2.3005
Benzene	5.2729	2.2829
Acetone	5.3167	2.3274

279 **4.5 Global Chemical Indices**

280 The global chemical indices such as chemical hardness, chemical softness, chemical potential,
281 electronegativity and electropilicity index of the molecule in the gas phase and in different
282 solvents were computed and reported in Table 5 using the frontier molecular orbital energy.

283 **Table 6:** Global chemical indices of the optimized Perylene in the gas phase and in different
 284 solvents.

Solvents	η (eV)	S (eV)	χ (eV)	μ (eV)	ω (eV)
Gas Phase	1.4968	0.6680	3.7725	-3.7725	4.7540
Water	1.4948	0.6690	3.8279	-3.8279	4.9013
Chloroform	1.4937	0.6695	3.7942	-3.7942	4.8188
Benzene	1.4950	0.6689	3.7772	-3.7772	4.7734
Acetone	1.4947	0.6690	3.8221	-3.8221	4.8867

285
 286 Chemical hardness is proportional to the HOMO-LUMO energy gap. An Increase in the
 287 chemical hardness makes the molecule more stable and less reactive. As seen in Table 6,
 288 Perylene molecule **in the gas phase with slightly higher value of** chemical hardness of 1.4968eV
 289 is considered to be harder and more stable than in the rest of the solvents, followed by benzene,
 290 water and acetone with chemical hardness of 1.4950eV, 1.4948eV and 1.4947eV respectively.
 291 This indicates that Perylene in chloroform is more stable than in the rest of the solvents.
 292

293 **4.6 Thermodynamic Properties**

294 **Table 7 presents** the components and total contribution of the electronic, translational, rotational
 295 and vibrational energies to the entropy (S) and heat capacity (C_v) as well as the rotational
 296 constants and zero-point vibrational energies (ZPVE) of Perylene in the gas phase and in
 297 different solvents.

298 **Table 7:** Thermodynamic properties of the optimized structure of perylene in the gas phase and
 299 different solvents.

Gas Phase			Water		Chloroform		Benzene		Acetone	
Positions	C _v (Kcal/ Mol)	S (Kcal/ Mol)								
Electronic	0	0	0	0	0	0	0	0	0	0
Translational	2.981	42.47	2.981	42.47	2.981	42.47	2.981	42.47	2.981	42.47
Rotatio	2.981	33.24	2.981	33.24	2.981	33.24	2.981	33.24	2.981	33.24

nal		2		6		4		3		6
Vibrational	50.95 1	37.39 8	50.96 1	36.33 1	50.93 9	36.74 5	50.91 3	37.04 5	50.96 4	36.45 4
Total	56.91 3	113.1 14	56.92 2	112.0 51	56.90 1	112.4 63	56.87 5	112.7 62	56.92 5	112.1 74
Rotational Constants (GHz)		0.625 04	0.62372		0.62427		0.62464		0.62388	
		0.330 6	0.33026		0.33042		0.33056		0.33027	
		0.216 23	0.21593		0.21606		0.21616		0.21595	
ZPVE (Kcal/Mol)		158.5 5182	157.37117		157.80191		158.12372		157.48719	

300

301 It can be observed in Table 7 that specific heat capacity of perylene is found to increase with an
 302 increase in the polarity of the solvents, while the entropy decreases as the dielectric constant
 303 increases. The zero-point vibrational energy (ZPVE) decreases with an increase in the polarity of
 304 the solvents.

305

306 **4.7 Non-Linear Optical Properties**

307 Our investigation also highlighted the effects of solvents on the nonlinear optical properties of
 308 the molecule. This is necessary for sufficient understanding of the nonlinear optical response of
 309 the molecule. Nonlinear optical (NLO) effect arises from the interactions of electromagnetic
 310 fields in various media to produce new fields altered in phase, frequency, amplitude and other
 311 propagation characteristics from the incident fields [31].

312 **Table 8 presents** the non-linear optical properties in atomic mass unit (a.u) of perylene molecule
 313 in the gas phase and in solvents. The properties computed and reported are dipole moment (μ_{tot}),
 314 polarizability ($\langle\alpha\rangle$), anisotropic polarizability ($\Delta\alpha$) and hyperpolarizability (β_{tot}).

315 **Table 8:** Non-linear optical properties (in Debye) of the optimized perylene molecule in the gas
 316 phase and different solvents.

Solvents	μ_{tot}	$\langle\alpha\rangle$	$\langle\Delta\alpha\rangle$	β_{tot}

Gas Phase	0.0000	108.2104	24.4360	1.00 E-4
Water	0.0000	104.3552	31.0839	4.36 E-4
Chloroform	0.0000	105.9012	28.2349	3.00 E-4
Benzene	0.0000	107.0436	26.1246	1.41 E-4
Acetone	0.0000	104.6985	30.4309	2.83 E-4

317

318 The dipole moment in a molecule is an important electronic property which results from non-
 319 uniform distribution of charges on the various atoms in the molecule [21]. It can be observed in
 320 **Table 8 that perylene** is a neutral molecule with a dipole moment of **0.000eV both in the gas**
 321 **phase and in the solvents.** It can also be observed that the polarizability of Perylene increases as
 322 the polarity of the solvents decreases whereas the anisotropic polarizability increases with an
 323 increase in the polarity of the solvents. Consequently, increasing or decreasing the polarity of the
 324 solvents plays a significant role in determining the values of the non-linear optical properties of
 325 **perylene.**

326

327 **4.8 Natural Bond Orbital (NBO) Analysis**

328 Natural Bond Orbital (NBO) analysis provides an efficient method for studying intra-and inter-
 329 molecular interaction among bonds and also provides a convenient basis for investigating charge
 330 transfer or conjugative interactions in molecular systems. Table 9 **presents the results of Natural**
 331 **Bond Orbital analysis of the optimized structure of perylene molecule** in the gas phase and in
 332 different solvents.

333 **Table 9:** Natural Bond Orbital (NBO) of optimized perylene molecule in the gas phase and in
 334 different solvents.

Donor NBO (i)	Acceptor NBO (j)	$E^{(2)}$ Kcal/mol	E(j)-E(i) a.u	Fji a.u	Donor NBO (i)	Acceptor NBO (j)	$E^{(2)}$ Kcal/mol	E(j)-E(i) a.u	Fji a.u
Water					Chloroform				
σ C2-C5	σ^* C1-C2	1.40	1.18	0.036	σ C2-C5	σ^* C1-C3	4.29	1.16	0.052
σ C2-C5	σ^* C1-C4	4.03	1.18	0.062	σ C2-C5	σ^* C1-C4	3.88	1.16	0.060
σ C2-C5	σ^* C2-C7	2.81	1.22	0.052	σ C2-C5	σ^* C2-C5	3.27	1.10	0.054
σ^* C5- σ C2-C5	C11	2.33	1.16	0.046	σ C2-C5	σ^* C2-C7	4.49	1.21	0.066
σ^* C5- σ C2-C5	C12	3.74	1.20	0.057	σ C2-C5	σ^* C3-C8	2.27	1.23	0.047
σ C2-C5	σ^* C7-	1.95	1.21	0.044	σ C2-C5	σ^* C4-	2.41	1.18	0.048

	C14					C10			
σ C2-C5	σ^* C11-C20	2.66	1.22	0.049	σ C2-C5	σ^* C5-C12	2.30	1.23	0.048
σ C2-C5	σ^* C12-C21	1.87	1.20	0.042	σ C2-C5	σ^* C7-H16	2.37	1.11	0.046
σ C11-C20	σ^* C2-C5	2.61	1.13	0.049	σ C11-C20	σ^* C2-C5	3.10	1.09	0.052
σ C11-C20	σ^* C3-C6	2.58	1.11	0.048	σ C11-C20	σ^* C3-C6	2.91	1.09	0.050
σ C11-C20	σ^* C5-C11	4.04	1.17	0.062	σ C11-C20	σ^* C5-C11	3.07	1.16	0.053
σ C11-C20	σ^* C6-C11	3.89	1.17	0.060	σ C11-C20	σ^* C6-C11	3.36	1.15	0.056
σ C11-C20	σ^* C20-C27	2.69	1.20	0.051	σ C11-C20	σ^* C20-C27	3.73	1.18	0.060
σ C11-C20	σ^* C20-C28	2.71	1.20	0.051	σ C11-C20	σ^* C20-C28	3.72	1.18	0.060
σ C11-C20	σ^* C27-H31	2.35	1.11	0.046	σ C11-C20	σ^* C27-H31	1.81	1.10	0.040
σ C11-C20	σ^* C28-H32	2.36	1.11	0.046	σ C11-C20	σ^* C28-H32	1.85	1.10	0.041
Benzene					Gas Phase				
σ C1-C2	σ^* C1-C3	4.31	1.16	0.063	σ C1-C2	σ^* C1-C3	4.30	1.16	0.063
σ C1-C2	σ^* C1-C4	4.31	1.17	0.063	σ C1-C2	σ^* C1-C4	4.31	1.17	0.063
σ C1-C2	σ^* C2-C5	2.49	1.12	0.047	σ C1-C2	σ^* C2-C5	2.49	1.12	0.047
σ C1-C2	σ^* C2-C7	3.75	1.25	0.061	σ C1-C2	σ^* C2-C7	3.75	1.25	0.061
σ C1-C2	σ^* C3-C8	2.29	1.21	0.047	σ C1-C2	σ^* C3-C8	2.29	1.21	0.047
σ C1-C2	σ^* C4-C10	2.67	1.20	0.051	σ C1-C2	σ^* C4-C10	2.67	1.20	0.051
σ C1-C2	σ^* C5-C12	2.23	1.21	0.047	σ C1-C2	σ^* C5-C12	2.23	1.21	0.047
σ C1-C2	σ^* C7-H16	2.42	1.12	0.047	σ C1-C2	σ^* C7-H16	2.45	1.11	0.047
σ C11-C20	σ^* C2-C5	3.07	1.12	0.052	σ C11-C20	σ^* C2-C5	3.06	1.12	0.052
σ C11-C20	σ^* C3-C6	2.24	1.11	0.045	σ C11-C20	σ^* C3-C6	2.24	1.11	0.045
σ C11-C20	σ^* C5-C11	4.25	1.16	0.063	σ C11-C20	σ^* C5-C11	4.24	1.16	0.063
σ C11-C20	σ^* C6-C11	3.95	1.16	0.061	σ C11-C20	σ^* C6-C11	3.94	1.16	0.061
σ C11-C20	σ^* C20-C27	3.83	1.18	0.060	σ C11-C20	σ^* C20-C27	3.86	1.18	0.060
σ C11-C20	σ^* C20-C28	4.03	1.19	0.062	σ C11-C20	σ^* C20-C28	4.06	1.19	0.062
σ C11-	σ^* C27-	1.92	1.10	0.041	σ C11-	σ^* C27-	1.95	1.10	0.042

C20	H31				C20	H31			
σ C11-C20	σ^* C28-H32	1.80	1.10	0.040	σ C11-C20	σ^* C28-H32	1.83	1.10	0.040
Acetone									
σ C1-C2	σ^* C1-C3	4.30	1.16	0.063					
σ C1-C2	σ^* C1-C4	3.89	1.16	0.060					
σ C1-C2	σ^* C2-C5	3.27	1.10	0.054					
σ C1-C2	σ^* C2-C7	4.48	1.21	0.066					
σ C1-C2	σ^* C3-C8	2.27	1.23	0.047					
σ C1-C2	σ^* C4-C10	2.24	1.18	0.048					
σ C1-C2	σ^* C5-C12	2.31	1.23	0.048					
σ C1-C2	σ^* C7-H16	2.34	1.12	0.046					
σ C11-C20	σ^* C2-C5	3.11	1.09	0.052					
σ C11-C20	σ^* C3-C6	2.92	1.09	0.051					
σ C11-C20	σ^* C5-C11	3.07	1.16	0.053					
σ C11-C20	σ^* C6-C11	3.37	1.15	0.056					
σ C11-C20	σ^* C20-C27	3.71	1.18	0.060					
σ C11-C20	σ^* C20-C28	3.70	1.18	0.059					
σ C11-C20	σ^* C27-H31	1.78	1.10	0.040					
σ C11-C20	σ^* C28-H32	1.38	1.10	0.040					

335

336 The larger $E^{(2)}$ value, the more intensive is the interaction between electron donors and
 337 acceptors. The more donation tendency from electron donors to electron acceptors, the greater is
 338 the extent of conjugation of the whole system [23]. It can be seen from Table 9 that the largest
 339 value of stabilization (4.49 Kcal/mol) energy $E^{(2)}$ of perylene was obtained in chloroform.
 340 Hence, there is high intensive interactions between σ C1-C2 and σ^* C2-C7 and has greater
 341 conjugation in the molecule. The order of this interaction is more in
 342 Chloroform>Acetone>Benzene>Gas Phase>Water. This phenomenon occurs as the polarity
 343 decreases between chloroform and benzene.

344

345 **5. CONCLUSION**

346 To understand the effects of solvents on structural, electronic, thermodynamic and non-linear
347 optical properties of Perylene molecule, we have carried out an extensive computational study of
348 the HOMO, LUMU, HOMO-LUMO energy gap, ionization potential, electron affinity, chemical
349 hardness, chemical softness, chemical potential, electronegativity, electrophilicity index, dipole
350 moment, polarizability, anisotropic polarizability, hyperpolarizability, entropy, heat capacity,
351 rotational constants and zero-point vibrational energy using the B3LYP methods under 6-
352 311++G(d,p) basis set.

353 In the structural properties calculations, Our findings revealed that the bonds of perylene tend to
354 be stronger in the gas phase and in solvents compared to that of an isolated perylene as reported
355 in the literature. It was observed that the bond lengths increases with an increase in the polarity
356 of the solvents, while the bond angles were found to increase as the polarity of the solvents
357 decreases. In the global quantities calculations, it was found that the electron transfer from
358 HOMO to LUMO was found to be relatively easier in chloroform than in the gas phase an in the
359 rest of the solvents. The global quantities, HOMO and HOMO-LUMO energy gaps were found
360 to increase as the polarity of the solvents increases. The ground state energy of perylene
361 increases with decrease in polarity of the solvents.

362 In the Thermodynamic part of our work the specific heat capacity of Perylene increases with an
363 increase in the polarity of the solvents while the entropy and the zero-point vibrational energy
364 decreases as the polarity of the molecule increases. In the non-linear optical properties
365 calculations, the polarizability increases with decrease in the dielectric constant of the solvents
366 while the anisotropic polarizability increases as the polarity of the solvents increases. In the NBO
367 analysis, high intensive interaction between donor and acceptor electrons was observed in
368 chloroform due to large value of stabilization energy. The results also show that careful selection
369 of basis set and solvents can be utilized to tune the optoelectronic properties of Perylene. The
370 same investigation should be carried out in future for neutral and charged perylene molecule.

371 **References**

372 [1] T. Rangel, A. Rinn, S. Sharifzadeh, H. Felipe, A. Pick, and S. G. Louie, “Low-lying
373 excited states in crystalline perylene,” *PNAS*, vol. 115, no. 2, pp. 284–289, 2018.

374 [2] M. Burian, F. Rigodanza, H. Amenitsch, L. Almásy, I. Khalakhan, Z. Syrgiannis, and M.
375 Prato, "Structural and Optical Properties of a Perylene Bisimide in Aqueous Media,"
376 *Chem. Phys. Lett.*, 2017, 683, 454-458..

377 [3] P. Taylor and J. D. Myers, "Organic Semiconductors and their Applications in
378 Photovoltaic Devices Organic Semiconductors and their Applications in Photovoltaic
379 Devices," *Polym. Rev.*, 2012 52(1), 1-37.

380 [4] J. Calbo, A. Doncel, G. Juan, and A. Enrique, "Tuning the optical and electronic
381 properties of perylene diimides through transversal core extension," *Theor. Chem. Acc.*,
382 vol. 137, no. 27, pp. 1–11, 2018.

383 [5] G. Malloci, G. Cappellini, G. Mulas, and A. Mattoni, "Electronic and optical properties of
384 families of polycyclic aromatic hydrocarbons: A systematic (time-dependent) density
385 functional theory study," *Chem. Phys.*, vol. 384, no. 1–3, pp. 19–27, 2011.

386 [6] M. Mohamad, R. Ahmed, A. Shaari, and S. G. Said, "Structure - dependent optoelectronic
387 properties of perylene , di - indenoperylene (DIP) isolated molecule and DIP molecular
388 crystal," *Chem. Cent. J.*, pp. 1–9, 2017.

389 [7] A. Furube, M. Murai, Y. Tamaki, S. Watanabe, and R. Katoh, "Effect of Aggregation on
390 the Excited-State Electronic Structure of Perylene Studied by Transient Absorption
391 Spectroscopy," pp. 6465–6471, 2006.

392 [8] I. A. Fedorov, "Structure and electronic properties of perylene and coronene under
393 pressure : First-principles calculations," *Comput. Mater. Sci.*, vol. 139, pp. 252–259, 2017.

394 [9] I. A. Fedorov, Y. N. Zhuravlev, V. P. Berveno, I. A. Fedorov, Y. N. Zhuravlev, and V. P.
395 Berveno, "Structural and electronic properties of perylene from first principles
396 calculations Structural and electronic properties of perylene from first," *J. Chem. Phys.*,
397 vol. 94509, no. 138, pp. 1–6, 2013.

398 [10] A P. Maharolkar, A.G. Murugkar, P.W. Khirade, S.C. Mehrotra, "Study of thermophysical
399 properties of associated liquids at 308.15 K and 313.15 K", *Russian Journal of Physical
400 chemistry A* , 91 (9), 1710-1716, 2017.

401 [11] D. Sholl, Density Functional Theory: A Practical Introduction. Hoboken, New Jersey:
402 John Wiley & Sons, Inc, Pp. 1, 2009.

403 [12] P. Giannozzi, “Lecture Notes Per Il Corso Di Struttura Della Materia (Dottorato Di Fisica
404 , Universit ` A Di Pisa , V . 2005): Density Functional Theory For Electronic Structure
405 Calculations,” Pp. 1–35, 2005.

406 [13] P. H. and W. Kohn, “Inhomogeneous Electron Gas,” *Phys. Rev.*, vol. 136, no. 3B, pp.
407 864–870, 1964.

408 [14] R. M. Martin, Electronic Structure, Basic Theory And Practical Methods. Cambridge:
409 Cambridge University Press, Pp. 119, 2004.

410 [15] R. O. Jones, “Introduction to Density Functional Theory and Exchange-Correlation
411 Energy Functionals,” *Comput. Nanosci.*, vol. 31, pp. 45–70, 2006.

412 [16] O. E. Oyeneyin, “Structural and Solvent Dependence of the Electronic Properties and
413 Corrosion Inhibitive Potentials of 1 , 3 , 4-thiadiazole and Its Substituted Derivatives- A
414 Theoretical Investigation,” *Phys. Sci. Int. J.*, vol. 16, no. 2, pp. 1–8, 2017.

415 [17] M. F. Khan, R. Bin Rashid, A. Hossain, and M. A. Rashid, “Computational Study of
416 Solvation Free Energy, Dipole Moment, Polarizability, Hyperpolarizability and Molecular
417 Properties of Betulin , a Constituent of *Corypha taliera* (Roxb .),” *Dhaka Univ. J. Pharm.*
418 *Sci.*, vol. 16, no. 1, pp. 1–8, 2017.

419 [18] K. K. Srivastava, S. Srivastava, and T. Alam, “Theoretical study of the effects of solvents
420 on the ground state of TCNQ,” *Pelagia Res. Libr.*, vol. 5, no. 1, pp. 288–295, 2014.

421 [19] M. Targema, M. D. Adeoye, and S. T. Gbangban, “Calculation of Electronic Properties of
422 Some 4-Nitroaniline Derivatives : Molecular Structure and Solvent Effects,” *Int. Res. J.*
423 *Pure Appl. Chem.*, vol. 8, no. 3, pp. 165–174, 2015.

424 [20] H. Abdulaziz, A. S. Gidado, A. Musa, and A. Lawal, “Electronic Structure and Non-
425 Linear Optical Properties of Neutral and Ionic Pyrene and Its Derivatives Based on
426 Density Functional Theory,” *J. Mater. Sci. Rev.*, vol. 2, no. 3, pp. 1–13, 2019.

427 [21] D. Pegu, "Solvent Effects on Nonlinear Optical Properties of Novel Para-nitroaniline
428 Derivatives : A Density Functional Approach," *Int. J. Sci. Res.*, vol. 3, no. 7, pp. 469–474,
429 2014.

430 [22] R. P. Gangadharan, "First Order Hyperpolarizabilities , NPA and Fukui Functions . . .,"
431 *ACTA Phys. POLANICA A*, vol. 127, no. 3, pp. 748–752, 2015.

432 [23] Z. Rui-zhou, L. Xiao-hong, and Z. Xian-zhou, "Molecular structure , vibrational spectra
433 and NBO analysis on using DFT method," *Indian J. Pure Appl. Phys.*, vol. 49, no. 11, pp.
434 731–739, 2011.

435 [24] A. D. Becke and A. D. Becke, "Densityfunctional thermochemistry . III . The role of exact
436 exchange Density-functional thermochemistry . III . The role of exact exchange," *J.
437 Chem. Phys.*, vol. 98, no. 7, pp. 5648–5652, 1993.

438 [25] R. G. P. Chengteh Lee, Weitao Yang, "Developmenet of the ColleSalvetti Correlation-
439 Energy Formula into a Functional of the Electron Density," *Phys. Rev. B*, vol. 37, no. 2,
440 pp. 785–789, 1988.

441 [26] H. M. Frisch M. J., Trucks G. W., Schlegel H. B., Scuseria G. E., Robb M. A., Cheeseman
442 J. R., Scalmani G., Barone V., Mennucci B., Petersson G. A., Nakatsuji H., Caricato M.,
443 X. Li, H. Hratchian P., Izmaylov A. F., Bloino J., Zheng G., Sonnenberg J. L., "Gaussian
444 Software." Gaussian, INC, 2004.

445 [27] F. Glendening, E., D., Reed, A., B., Carpenter, J., E. and Wienhold, "NBO 3.1."
446 University of Wisconsin, Madison, 1998.

447 [28] S. Suzuki, Y. Morita, K. Fukui, K. Sato, D. Shiomi, T. Takui, and K. Nakasuji,
448 "Aromaticity on the Pancake-Bonded Dimer of Neutral Phenalenyl Radical as Studied by
449 MS and NMR Spectroscopies and NICS Analysis," *J. Am. Chem. Soc.*, vol. 128, no. 8, pp.
450 2530–2531, 2006.

451 [29] A. H. Mekky, H. G. Elhaes, M. M. El-okr, A. S. Al-aboodi, and M. A. Ibrahim, "Applied
452 & Computational Mathematics Effect of Solvents on the Electronic Properties of
453 Fullerene Based Systems : Molecular Modelling," *Applies Comput. Math.*, vol. 4, no. 1,

454 pp. 1–4, 2015.

455 [30] A. Kumer, B. Ahmed, A. Sharif, and A. Al-mamun, “A Theoretical Study of Aniline and
456 Nitrobenzene by Computational Overview,” *Asian J. Phys. Chem. Sci.*, vol. 4, no. 2, pp.
457 1–12, 2017.

458 [31] C. Janaki, E. Sailatha, S. Gunasekaran, and G. R. R. Kumaar, “Molecular structure and
459 spectroscopic characterization of Metformin with experimental techniques and DFT
460 quantum chemical calculations,” *Int. J. Techno. Chem. Res.*, vol. 2, no. 2, pp. 91–104,
461 2016.

462

463